JOURNAL OF MATERIALS SCIENCE 19 (1984) 723–736

X-ray diffraction radial distribution function studies on bone mineral and synthetic calcium phosphates

M. D. GRYNPAS,* L. C. BONAR, MELVIN J. GLIMCHER
Laboratory for the Study of Skeletal Disorders and Rehabilitation, Department of Orthopaedic Surgery, Harvard Medical School, Childrens Hospital Medical Center, 300 Longwood Avenue, Boston, Massachusetts 02115, USA

An investigation of the molecular structure of bone mineral and synthetic calcium phosphates was carried out using radial distribution function (RDF) techniques. The X-ray data were collected using Cu$K\alpha$ and Mo$K\alpha$ radiation to insure the validity of the RDFs. Synthetic preparations of hydroxyapatite (HA) varying in their crystal size and crystallinity, and amorphous calcium phosphate (ACP), were studied, as well as bone samples from a 1-year-old chicken and 16-day embryonic chicks. Mixtures of embryonic bone and synthetic ACP were also investigated. The RDFs of bone and crystalline HA samples are similar in peak position, and show evidence of an atomic order extending to 2.5 nm and beyond. The RDF of ACP differs from that of HA, showing only short range order up to 0.9 nm, as well as small differences in peak shape. The decrease in intensity of the RDF function with increasing distance (r), observed with both HA and bone samples can be related to a decrease in crystallinity and crystal size. The RDF data indicate there is no significant amount of ACP in either very young or mature bone. The RDFs of the embryonic bone + synthetic ACP mixtures showed that a small amount of ACP can be readily detected in a sample of bone with a poorly crystalline mineral phase; from this we estimate the threshold for detection of ACP in bone to be 12% or less.

1. Introduction

The mineral component of bone is known to be a poorly crystalline apatite with a composition most closely approximating hydroxyapatite, but with significant amounts of CO_3^{2+} and H^+ contaminant ions adsorbed on and/or incorporated in the crystallites, and with a deficiency in Ca^{2+}. As bone matures and ages, the mineral becomes more crystalline, as shown by X-ray diffraction (XRD) or infrared spectroscopy (IR), the H^+ content decreases and the Ca^{2+} content increases toward the stoichiometric value [1–3]. Posner and his co-workers suggested that, in addition to the readily identifiable apatitic phase, bone mineral contains an amorphous calcium phosphate (ACP) phase [4–6]. They proposed that ACP was the initial phase formed in the early stages of mineralization, and that it converted to the apatitic phase on maturation. Based on comparison of X-ray diffraction intensities from bone and synthetic crystalline hydroxyapatite (HA) standards, they estimated that the mineral of young bones contained 50% or more ACP, and that of mature bones 25 to 30% ACP [7, 8]. The ACP hypothesis of bone development has been widely accepted and a number of workers have measured the apparent ACP content of bone and other mineralized tissues [8–14], or studied the effect of various substances and conditions on the precipitation of ACP or its conversion to apatite *in vitro* [15–17].

Posner and Betts [18, 19] used radial distribution function (RDF) analysis of XRD data in an

*Present address: Mount Sinai Hospital, 600 University Avenue, Toronto, Ontario M5G 1X5, Canada.

0022–2461/84 $03.00 + .12

attempt to find positive evidence for the existence of ACP in bone. They studied relatively mature rabbit bone from which the organic matrix had been removed by treatment with hydrazine, which, from diffracted-intensity comparison, would be expected to have an apparent ACP content of 30 to 35%. They could find no evidence of an amorphous phase in this bone and, because of uncertainties inherent in the RDF technique, they concluded that no more than 10% ACP could be present in the bone studied.

Because of the uncertainty regarding the existence and amount of ACP in bone mineral and its possible role in bone development, we have undertaken a thorough study to determine if ACP exists in bone mineral, and if so, how much is present at various stages of development and maturation [20, 21]. In the present investigation, we have extended the use of the RDF technique to the newly-formed bone of embryonic chicks. Although such bone would be expected to be predominantly ACP, we find no evidence for ACP, using the decrease in modulation of the RDF function $G(r)$ with increasing r as a criterion for the presence of an amorphous constituent. To assess the ability to detect ACP in the presence of apatitic bone mineral, we prepared mixtures of synthetic ACP and embryonic chick bone and find we can readily detect the presence of 12.5% ACP added to bone. We have also studied bone of a wide range of age and degree of maturity, and find no evidence consistent with the decrease in proportion of an amorphous component with age.

In addition, we have determined the RDFs of synthetic ACP, and of several synthetic HAs of varying degree of crystallinity.

And lastly, we have determined RDFs using both Cu$K\alpha$ and Mo$K\alpha$ radiation, in an attempt to ensure against artifacts in the RDFs due to series-termination errors.

We conclude from these studies that there is no detectable ACP even in very young bone, nor is there any indication of a change in proportion of any amorphous constituent with age. Since 12% ACP added to embryonic bone is readily detectable, ACP cannot play the role in bone formation and development previously ascribed to it.

2. Materials and methods

The following synthetic samples were prepared and used in this study.

1. Highly crystalline hydroxyapatite (HA1), which was prepared by slow precipitation from CO_2-free solutions of $CaCl_2$ and KH_2PO_4 at pH 9.0 to 9.5 at boiling temperature, following which the precipitate was filtered, washed with deionized water then refluxed for 45 days with frequent changes of H_2O, dried at 105° C and stored in a desiccator.

2. A less crystalline hydroxyapatite (HA2) which was formed by hydrolysis of an ACP [6] for 24 h in water kept at pH 7.0 to 8.0 by adding NH_4OH. The precipitate was washed in ethanol then dried at 65° C and stored in a desiccator.

3. A very poorly crystalline apatite (HA3) obtained by spontaneous conversion of an ACP precipitate over a period of a few weeks.

4. ACP prepared by mixing 0.016 M $CaCl_2$ with 0.01 M $(NH_4)_2HPO_4$ in water with ammonia to keep the pH about 10.5. The precipitate was then washed in ammonia water at 4° C, lyophilized and stored in a desiccator.

The biological samples were:

(a) the mid-diaphyses of the tibiae of 16-day-old chick embryos. Two separate preparations were made in order to assess reproducibility;

(b) the mid-diaphyses of the tibiae of 1-year-old postnatal chickens. The bone samples were removed immediately after sacrifice and cleaned of periosteum and adherent soft tissue. The mid-diaphysis was cut free and split, and the marrow was removed by scraping. The bones were then frozen in liquid nitrogen. Larger bones were broken into small (5 mm) pieces before freezing. The frozen bone samples were lyophilized, then pulverized in a percussion mill (Spex Freezer Mill, Model 6700) in liquid nitrogen. The bones were reduced to a 1 to 10 μm particle size range, with an average of 5 μm. Bone recovery was greater than 90%.

Mixtures of the mid-diaphyses of 16-day embryonic chick tibiae and ACP were made in the following proportions (by weight): (a) 75% 16-day chick bone and 25% ACP (3:1 mixture), and (b) 87.5% 16-day chick bone and 12.5% ACP (7:1 mixture).

All preparations were dried overnight at 105° C before chemical analysis. Samples were digested in hot 4:1 $HNO_3/HClO_4$. Calcium was determined by atomic absorption and phosphorus by the method of Dryer *et al.* [22]. The densities of the bone samples were calculated assuming a density of 3.15 g cm^{-3} for the inorganic fraction (Ca + PO_4) and a density of 1.35 g cm^{-3} for the organic frac-

tion. The densities used for the synthetic samples were either the theoretical value for HA (3.12 g cm^{-3}) or those calculated from measurements of the mass and volume of compressed pellets of the HA3 and ACP samples.

X-ray diffraction data were taken with Cu$K\alpha$ and Mo$K\alpha$ radiation on a Norelco Philips vertical diffractometer equipped with a graphite-crystal diffracted-beam monochromator. A scintillation counter detector connected to standard counting electronics was used to record the diffracted intensities on punched paper tape. Conventional Bragg–Brentano geometry was used with incident beam divergence of 1/4°, 1/2°, 1° or 4°, depending on the angular range scanned. The various slit ranges were overlapped to allow for internal scaling. The diffractometer was operated in the step scan mode with 10 000 counts/step, to give counting statistical precision of 1%. For Cu$K\alpha$, diffracted intensity measurements were made from 4.6° to 149.6° 2θ at 0.2° increments, with a 0.46 mm receiving slit (equivalent to 0.15° 2θ). For Mo$K\alpha$ radiation, measurements were made from 4.5° to 135° 2θ at 0.1° increments with a 0.23 mm (0.075° 2θ) receiving slit.

The X-ray diffraction data were corrected for instrument background (determined by measuring scattered intensity at each angle with an empty specimen holder) and scaled. The diffuse small-angle scattering below $K = 0.07\ nm^{-1}$ was eliminated by linear extrapolation from the measured intensity at $K = 0.07\ nm^{-1}$ to 0 at $K = 0$. The measured intensities were then corrected for absorption (A) and polarization (P) using expressions appropriate to the Bragg–Brentano geometry [23], and the corrected intensity $I(K)_{corrected}$ determined according to Equation 1:

$$I(K)_{corrected} = (I(K)_{measured} - I(K)_{background})/(PA). \quad (1)$$

The corrected intensities were then normalized to an absolute scale by means of Equation 2 [24], where $I_a(K)$ is the coherent scattering per atom in absolute units, and β is the normalization constant. The normalization constant was determined by the high angle [25], the RDF [26] and Norman [27] methods; a weighted average of the high angle and RDF values was used for further calculations.

$$I_a(K) = \beta I_{corrected}(K) - I_{eu}inc(K) \quad (2)$$

I_{eu}inc is the weighted sum of Compton scattering for the constituent Ca, P, O, C, and N atoms [12]. This coherent scattering normalized to the mean atomic scattering factors of the system gives the interference function [24].

$$I(K) = \frac{I_a(K) - (\langle f^2 \rangle - \langle f \rangle^2)}{\langle f \rangle^2} \quad (3)$$

where $I(K)$ is the total interference function, $\langle f \rangle$ and $\langle f^2 \rangle$ are the mean and mean-square scattering factors. The atomic scattering factors for Ca, P, O, N, and C, and dispersion corrections for Ca and P used are those of Doyle and Turner [28] and Cromer and Waber [29].

$I(K)$ can be written as:

$$I(K) = 1 + \int_0^\infty 4\pi r^2[\rho(r) - \rho_0] \frac{\sin Kr}{Kr} dr, \quad (4)$$

where $\rho(r)$ is the mean atomic number density at a distance r from an arbitrary origin and ρ_0 the average atomic number density in the sample.

For the actual Fourier transformation, a reduced interference function $F(K)$ is defined:

$$F(K) = K(I(K) - 1). \quad (5)$$

The Fourier transform of $F(K)$ gives the reduced radial distribution function, or atomic distribution function $G(R)$, the atomic density as a function of atomic separation.

$$G(r) = 4\pi r[\rho(r) - \rho_0] = \frac{2}{\pi} \int_0^\infty F(K) \sin Kr\, dK. \quad (6)$$

Finally, the RDF, which is defined as the number of ions in a spherical shell of radius r and unity thickness, expressed as a function of r, is given by:

$$RDF(r) = 4\pi r^2 \rho(r) = rG(r) + 4\pi r^2 \rho_0. \quad (7)$$

A computer program [24] was employed first to calculate the interference functions from the measured intensities, and then to calculate the Fourier transform to yield the atomic distribution function.

Errors may occur in the calculation of the RDF function due to the inaccuracy of the absorption correction, the normalization function, and to termination effects in the Fourier transformation, as discussed by Kaplow *et al.* [31, 31], Wagner [24], and Townsend and Ergun [32]. The error due to the absorption correction results in a spurious maximum below 0.1 mm and spurious ripples or subsidiary maxima in $G(r)$; we experimentally

adjusted the sample thickness parameter *TS* (see Table II), the effective diffracting thickness of the sample, to minimize these effects in the $G(r)$ function. With Cu$K\alpha$ diffraction data, this procedure was sufficient to yield clean $G(r)$s with consistent peak positions and only very small peaks below $r = 0.1$ nm. We could not sufficiently reduce the $r < 0.1$ nm peak in the $G(r)$s calculated from Mo$K\alpha$ diffraction data by this technique. Accordingly, we extrapolated $G(r)$ below $r = 1.0$ nm linearly to 0 at $r = 0$. The resulting $G(r)$ was then Fourier transformed, and the resultant transform (analogous to $F(K)$) was back-transformed to yield a modified $G(r)$, with the $r < 0.1$ nm peak, and any associated ripple, removed. All three normalization techniques (high-angle, RDF, and Krogh–Moe–Norman) yielded very similar values for the normalization constants (see Table II). Since all three techniques are based on different physical principles, we conclude from this similarity that the normalization procedure used is essentially correct.

Finally, by using an artificial temperature factor of the form $\exp(-\beta K^2)$ ($\beta = 0.05$) only with the data collected with Mo$K\alpha$ radiation to dampen the $F(K)$ function for $K > 8$, we prevent ripples and subsidiary maxima in the $G(r)$ function. (This procedure was not required in the data collected with copper radiation.) Despite these minor differences in treatment between the copper and molybdenum data, the resulting radial distribution functions are strikingly similar in peak position. Remaining small differences between the functions will be discussed later.

In order to estimate crystallite size in the various synthetic preparations and in the bone samples the values of β_{002}, the half-width at maximum height of the hydroxyapatite [0 0 2] reflection, were measured on computer-drawn graphs of the X-ray intensity measurements. Because instrumental broadening was small compared to sample peak breadth, measured half-widths were corrected for instrumental broadening by subtracting the square of β_{002} for a fully crystalline mineral fluorapatite from the square of the sample value and taking the square root of the difference. From these measurements the D values were calculated from the Sherrer equation [23]:

$$D = \frac{K\lambda}{\beta_{1/2} \cos\theta} \tag{8}$$

where λ is the X-ray wavelength and θ the diffraction angle. $\beta_{1/2}$ is the breadth at half-height of the peak, and K is a constant approximately equal to 1, but varying slightly with crystal habit; it was chosen as 0.9 for the elongated crystallites of bone and hydroxyapatite. The measurement based on the width at half the maximum height of the [0 0 2] peak corrected for instrumental broadening does not take into consideration the lattice strain effect; however, it will give an estimate of the average size of the long axis (c-axis) of these needle or plate-like crystals. The crystallinity, which represents a composite of all the factors affecting the size and perfection of the crystals [2] is not measured completely by line broadening.

3. Results

Table I presents the composition data of the samples used in this study. In the synthetic samples the difference between the total mass and the calcium + phosphate content can be attributed to water and extraneous ions adsorbed on the surface of the crystallites and ACP particles [2]. In the bone samples the difference between total mass and calcium phosphate content is due mostly to the organic matrix (mainly collagen) which decreases with age (Table I).

Table II presents the parameters used in the calculation of the RDF functions. It can be seen that the difference between the various independently derived normalization constants and the average used in our calculation is only a few percent, which gives us confidence that we have minimized the

TABLE I Chemical composition of synthetic calcium phosphate and bone samples

	Ca (% dry wt)	P (% dry wt)	Ca + PO_4 (% dry wt)	Ca/P (molar)
ACP	33.1	17.5	86.6	1.5
HA1	39.8	18.5	99.8	1.7
HA2	32.0	14.6	76.7	1.7
HA3	30.0	17.8	84.6	1.3
16-day embryonic chick bone	17.8	9.6	47.3	1.4
1-year chicken bone	26.2	12.6	64.8	1.6

TABLE II Normalization constants (from $K = 5$) and TS for Cu X-ray data

Sample	TS (cm)	HAC (10^{-2})	RDF (10^{-2})	RR (10^{-2})	N (10^{-2})	Ave. (10^{-2})
Synthetic preparations:						
HA1	0.0015	0.331	0.341	0.340	0.339	0.336
HA2	0.0015	0.364	0.383	0.384	0.385	0.374
HA3	0.0030	0.696	0.726	0.728	0.736	0.711
ACP	0.0030	0.617	0.638	0.640	0.645	0.628
Bone:						
1 year	0.0025	0.425	0.445	0.446	0.450	0.435
16 day	0.0040	0.402	0.417	0.417	0.419	0.409
7:1 mix	0.0050	0.384	0.394	0.394	0.392	0.389
3:1 mix	0.0040	0.491	0.508	0.507	0.506	0.500

HAC: high-angle constant [25]. RDF: RDF constant [26]. RR: reduced RDF constant [26]. N: original Norman constant [27]. Ave: average constant used to normalize the data. TS: specimen thickness used for absorption correction.

possible normalization errors and that the normalization procedure used is essentially correct.

Fig. 1 shows the interference function $I(K)$ of the synthetic calcium phosphates, determined with Cu$K\alpha$ radiation. $I(K)$ is the measured X-ray diffraction intensity after performing polarization, absorption, Compton and dispersion corrections and normalizing to the average scattering factor. The $I(K)$ of the ACP sample shows three major broad peaks often encountered in the diffracted

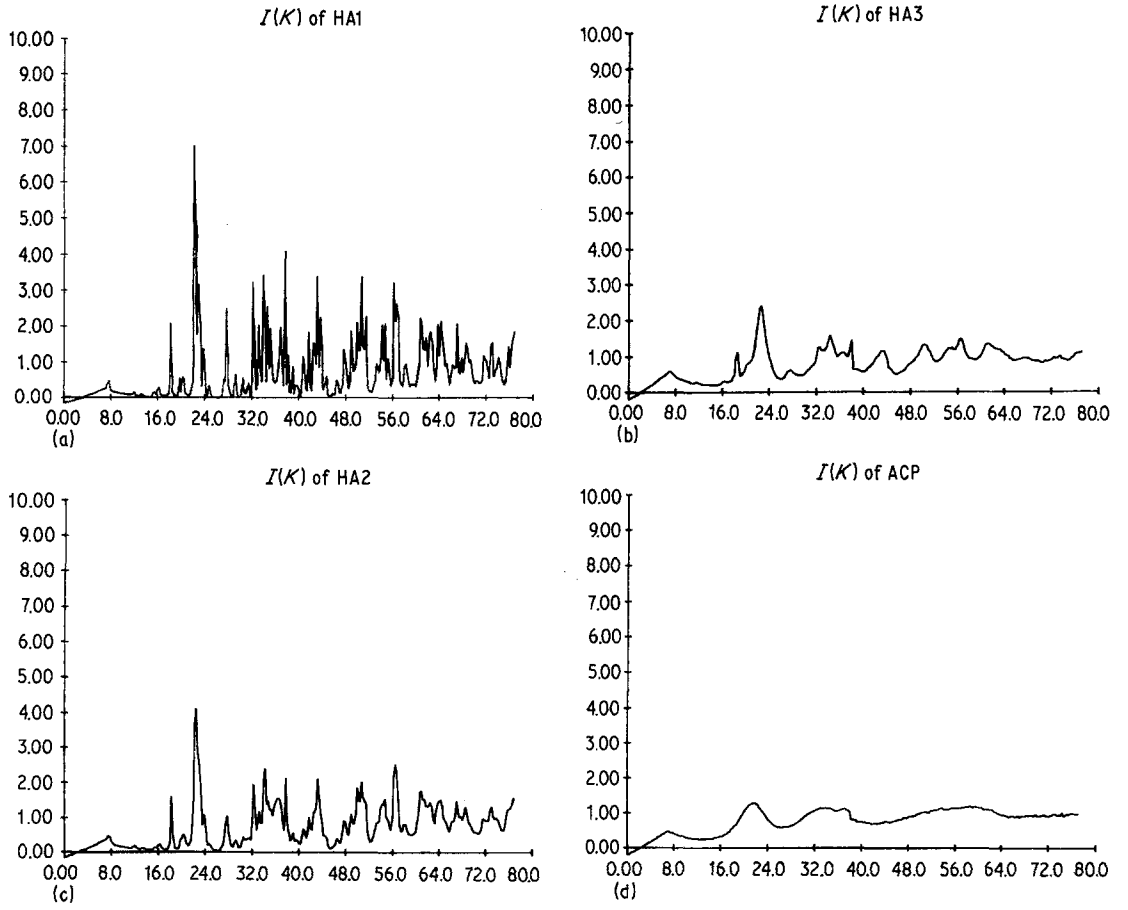

Figure 1 Interference functions [$I(K)$ against K in nm^{-1}] of various hydroxyapatite (HA) preparations and amorphous calcium phosphate (ACP). (The data were collected using copper radiation.)

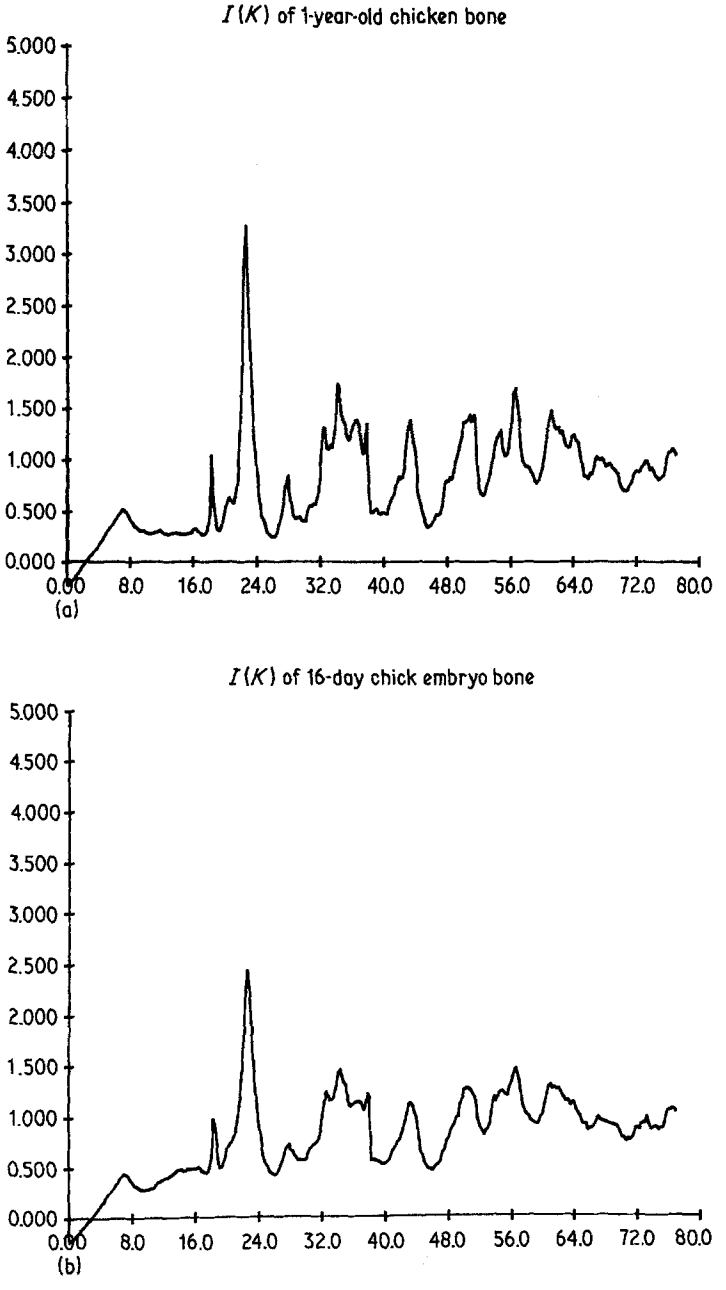

Figure 2 Interference functions [$I(K)$ against K in nm^{-1}] of 16-day chick embryo bone and 1-year-old chicken bone. (The data were collected using copper radiation.)

intensity from amorphous solids and liquids [33]. The three apatite samples, HA3, HA2, and HA1, are shown in order of increasing apparent crystallite size (HA3 = 14 nm, HA2 = 27.3 nm, and HA1 = 63.5 nm).

Fig. 2 shows $I(K)$ for the 1-year and 16-day embryo bones, similarly recorded with Cu$K\alpha$ radiation. It is evident from Fig. 2 and Table III that the apparent crystallite size of the 16-day embryo bone is similar to that of preparation HA3, and smaller than that of HA2. As expected, the amplitude of the $I(K)$ of the bone specimens (Fig. 2) lie between those of the HA3 and HA2 synthetic samples. This effect of crystallinity on the X-ray diffracted intensity is very marked: a three-fold decrease in $I(K)$ with decreased crystallinity.

The $I(K)$s of the two different preparations of chick embryo bones (16-day chick, 1- or 2- and 16-day chick 3) are practically indistinguishable. The two $I(K)$s derived from the two separate sets

TABLE III Modulation ratios (MR) and crystallite size (D)

Sample	MR (Cu)	MR (Mo)	D_{002}
Synthetic preparations:			
HA1	0.941	0.525	635A
HA2	0.699	–	273A
HA3	0.274	0.157	140A
ACP	0.075	0.052	–
Bone:			
1 year	0.415	0.238	160A
16 day (1)*	0.239	–	–
16 day (2)*	0.234	–	–
16 day (3)*	0.266	0.158	133A
7:1 mix	0.223	–	126A
3:1 mix	0.177	–	–

*16 day (1) and 16 day (2) are two measurements from the same sample preparation; 16 day (3) is another preparation of chick embryonic bone.

of XRD data from the first preparation of 16-day-old chick embryo bone are also indistinguishable. There is a greater difference between the two preparations of chick embryo bone than between the two runs of the same preparation, suggesting that biological variability (possibly due to small differences in age and maturation) may contribute a greater discrepancy than indeterminacies in the RDF determination (see Table III).

Fig. 3 shows the atomic distribution function $G(r)$ of the synthetic samples, calculated from Cu$K\alpha$ diffraction data. The modulation of the $G(r)$ of the ACP sample does not extend beyond about 0.9 nm, while the $G(r)$s of the three HA samples show modulation extending well beyond 2.5 nm, indicating ordering to this size range. The decreasing amplitude of the peaks with increasing r is an indication of the crystallinity of the samples;

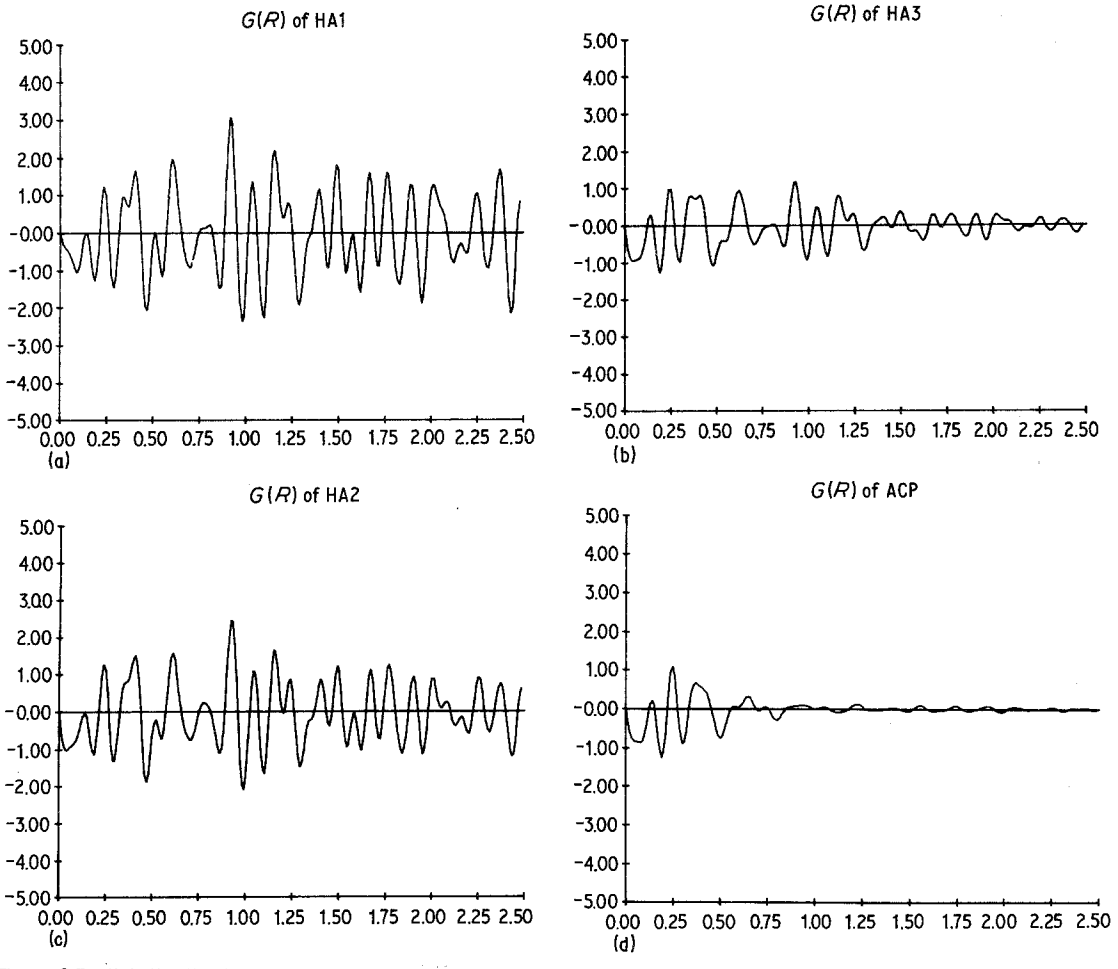

Figure 3 Radial distribution functions (RDFs) [$G(R)$ against R in nm] of various HA preparations and ACP calculated from data shown in Fig. 1.

the decrease is more extensive in the least crystalline sample, HA3, and is progressively less pronounced in the increasingly crystalline HA2 and HA1.

Fig. 4 shows the $G(r)$s of several of the same samples calculated from Mo$K\alpha$ diffraction data. Despite minor differences in peak intensities which can be attributed to the use of an artificial temperature factor and the residual effect of the suppressed peak below 0.1 nm, the $G(r)$ functions calculated from the molybdenum data are essentially similar to those calculated from the copper data.

In all the $G(r)$ functions, the peak at about 0.15 nm corresponds to the P–O bond distance of the tetrahedral phosphate (PO_4); the peak about 0.25 nm corresponds to the Ca–O and O–O distances, and the double peak between 0.3 and 0.5 nm corresponds to the Ca–Ca, P–P, and Ca–P distances in the HA structure [19]. Peaks above 0.5 nm cannot be assigned to unique atom pairs because of the many closely spaced next-nearest-neighbour interatomic distances encountered in such complex solids as calcium phosphates, where the distribution of six independent sets of interatomic vectors (Ca–Ca, P–P, O–O, Ca–O, P–P, and Ca–P) contribute to the RDF.

The $G(r)$ patterns of the bone samples are shown in Fig. 5, calculated from both copper and molybdenum diffraction data. They demonstrate a remarkable similarity among themselves and are also very similar to the $G(r)$s of the several HA samples examined in this study (cf. Figs. 3 and 4). This similarity indicates that the atomic environment in the bone mineral crystallite does not change very much with age, and that the atomic order extends to 2.5 nm and beyond.

In the embryonic bone patterns, the decrease in peak amplitude or modulation of $G(r)$ with increasing r is more pronounced than in the older bone; this can be attributed to the smaller crystal size and decreased crystallinity of the mineral crystallites in the embryonic bones. The decreased crystallinity of the embryonic bone mineral is a result of lattice substitution, extraneous ions, lattice strain, and a much greater surface to volume ratio which increases the relative importance of surface-bound extraneous ions and surface defects.

The effect of the organic component's contribution to the $G(r)$ of the bone samples shown in Fig. 5 is negligible, although it was included in the RDF calculation. This is true even in the $G(r)$ of embryonic bone, in which the organic material constitutes almost half the total weight. This results from the fact that the organic matrix contains only elements of low z (carbon, nitrogen, and oxygen) whose contribution to the X-ray scattering is much smaller than those of the heavier calcium and phosphorus atoms.

In Fig. 6 the $G(r)$ patterns of the 16-day chick bone and of a 3:1 mixture and of a 7:1 mixture of that same bone and ACP are shown. Adding ACP to the embryonic bone reduces the diffracted X-ray intensities. However, in the $G(r)$ function, the contribution of the ACP can only be detected below about 0.7 nm; above this, the only effect of the added ACP is to decrease the modulation of $G(r)$ relative to that of the bone alone.

To obtain a quantitative measure of the extent of modulation of $G(r)$ and the decrease in modulation with increasing r, we calculate the modulation ratio, defined as the ratio of the modulation (calculated as the root-mean-square (RMS) or square root of the variance) of $G(r)$, over the $0.1\,\text{nm} < r < 0.7\,\text{nm}$ range, to the modulation over the $1.5\,\text{nm} < r < 2.5\,\text{nm}$ range.

$$\text{MR} = \frac{\left[\sum_{r=15}^{25} \frac{G(r_n)^2}{n}\right]^{1/2}}{\left[\sum_{r=1}^{7} \frac{G(r_n)^2}{n}\right]^{1/2}}. \qquad (9)$$

In the region $0.1\,\text{nm} < r < 0.7\,\text{nm}$, virtually any material with even short-range order would contribute to modulation and crystal size has little effect. Over the region from 1.5 to 2.5 nm there should be no contribution due to the presence of ACP, and factors such as crystal size and crystallinity become significant. In theory, an ideally crystalline sample would be expected to have an MR close to 1, i.e. showing only a very slight decrease in modulation with increasing r. An amorphous sample would be expected to have an MR close to zero, because there is no contribution to modulation beyond 0.9 to 1.0 nm.

In Table III we list the modulation ratios of the samples we have studied, calculated from both copper and molybdenum data, together with their crystallite size, calculated from HA [0 0 2] diffraction line broadening. The MR of the highly crystalline HA1 was calculated to be 0.941, using Cu$K\alpha$ diffraction data, and that of ACP to be 0.075.

The MR ratios using the molybdenum data are

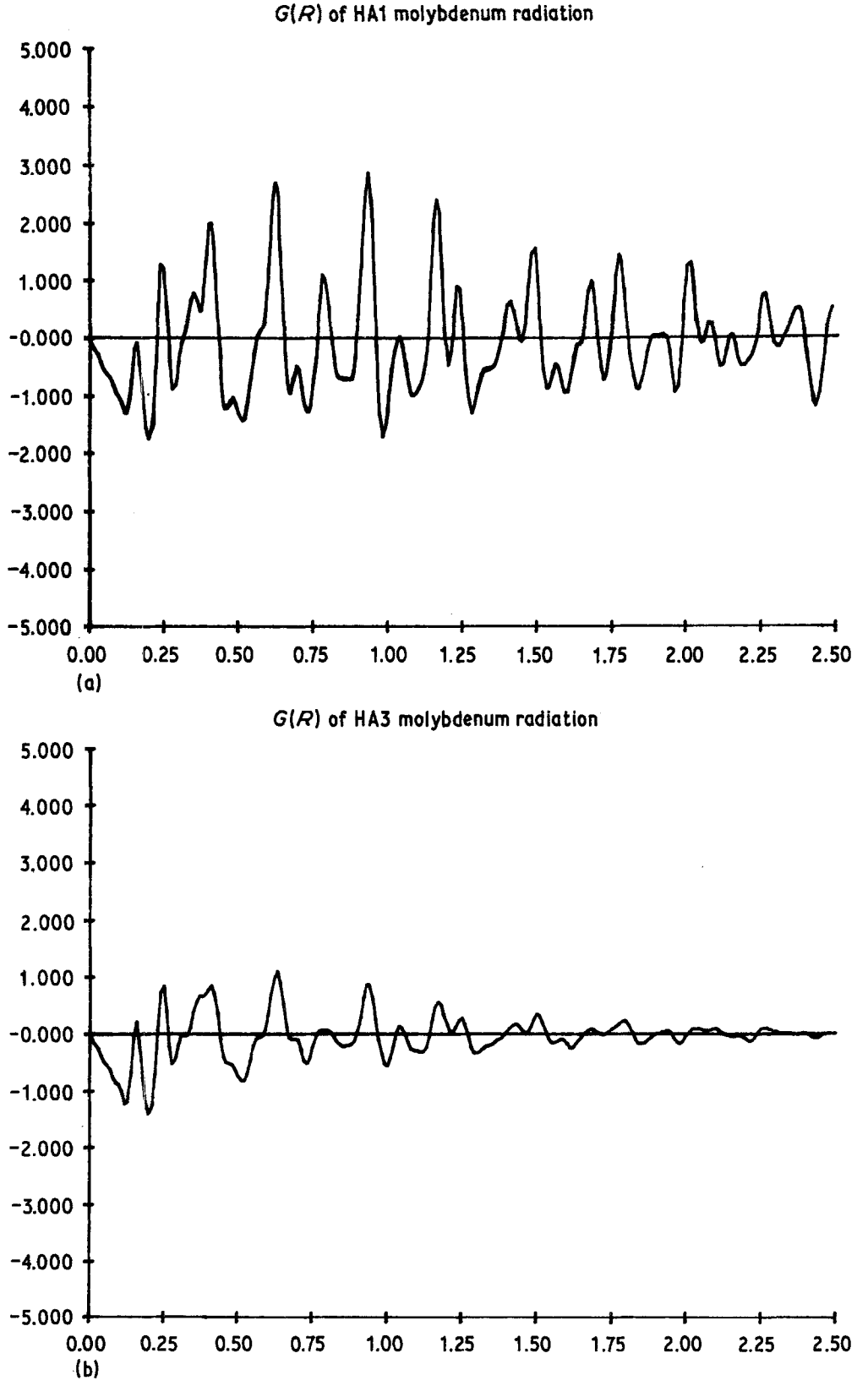

Figure 4 RDFs [$G(R)$ against R in nm] of various HA and ACP calculated from data collected with molybdenum radiation.

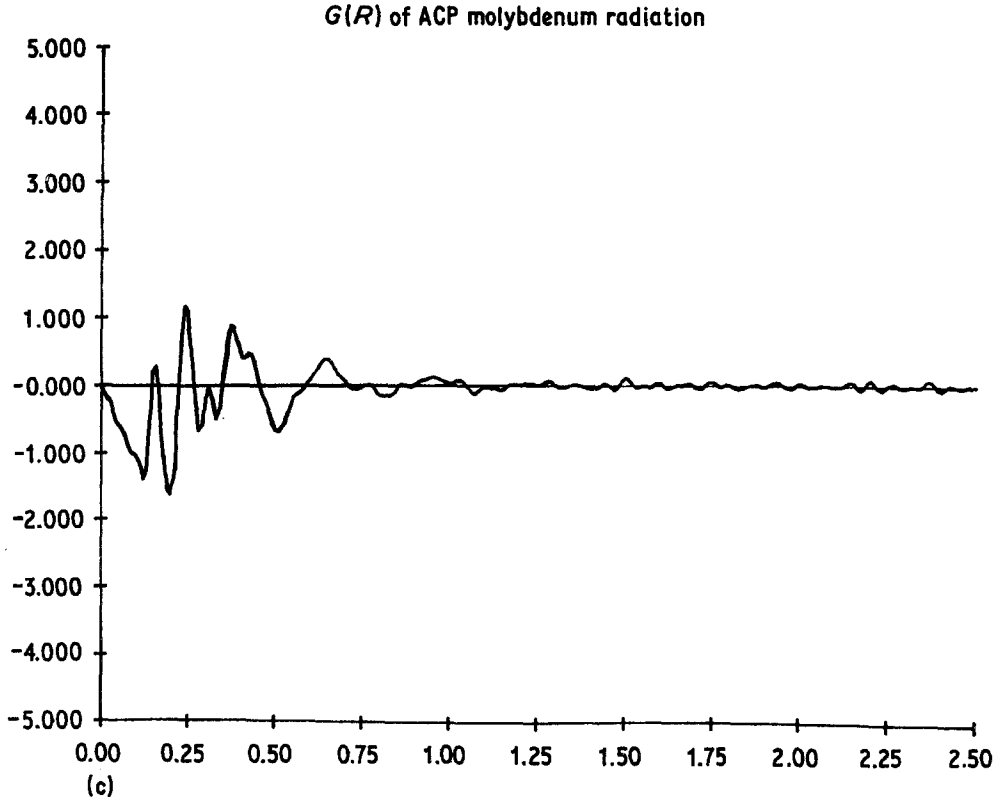

Figure 4 Continued.

somewhat lower because of the artificial temperature factor used for the data reduction. However, there is a strong linear correlation between MRs determined with copper data and those determined with molybdenum data, as shown in Fig. 7, which indicates that the two sets of data are essentially similar. The MRs of the two sets of diffraction data from the same preparation of embryonic bone are very close, demonstrating that the errors of the RDF methods are minimal, and the differences between two different preparations of embryonic bone are within 10% of each other. From the 3:1 and 7:1 mixture of 16-day chick embryo bone and ACP (Table III) it is clear that even 12.5% of ACP can be detected when mixed with the very young, embryonic bone.

4. Discussion

Townsend and Ergun [32] have previously used RDF analysis of XRD data to evaluate the extent of medium- to long-range order (up to 6 nm) in poorly crystalline materials. In the present report we use RDF analysis to estimate the extent of order of intermediate distances, approximately 0.6 to 2 nm, and in particular, to determine if any appreciable quantity of an amorphous phase lacking in intermediate as well as long-range order is present in bone mineral.

The decrease in modulation of $G(r)$ with increasing r, as measured by the MR, is a consequence of all the factors causing a departure from crystalline perfection, including small size, lattice strain, impurities, vacancies, and disorder, and the presence of a distorted layer at the crystallite surface. This latter effect is probably a very significant one in the synthetic samples of very small crystallite size studied here, as well as in bone: a crystallite of 15 nm x 5 nm x 5 nm, similar to the bone and synthetic sample of smallest crystallite size studied, will have 40% of its volume within 0.5 nm (the intermolecular distance between calcium and the nearest PO_4 group) of the surface. Diffraction line broadening measures the size and lattice strain components of the disorder, but the other components would be expected to vary similarly. The variations of MR with D_{002}, shown in Fig. 8, indicates that the MR of ACP is substantially lower than that of poorly crystalline HA crystallites, even HA with a D_{002} value comparable to that of very recently formed bone. Thus the presence of a

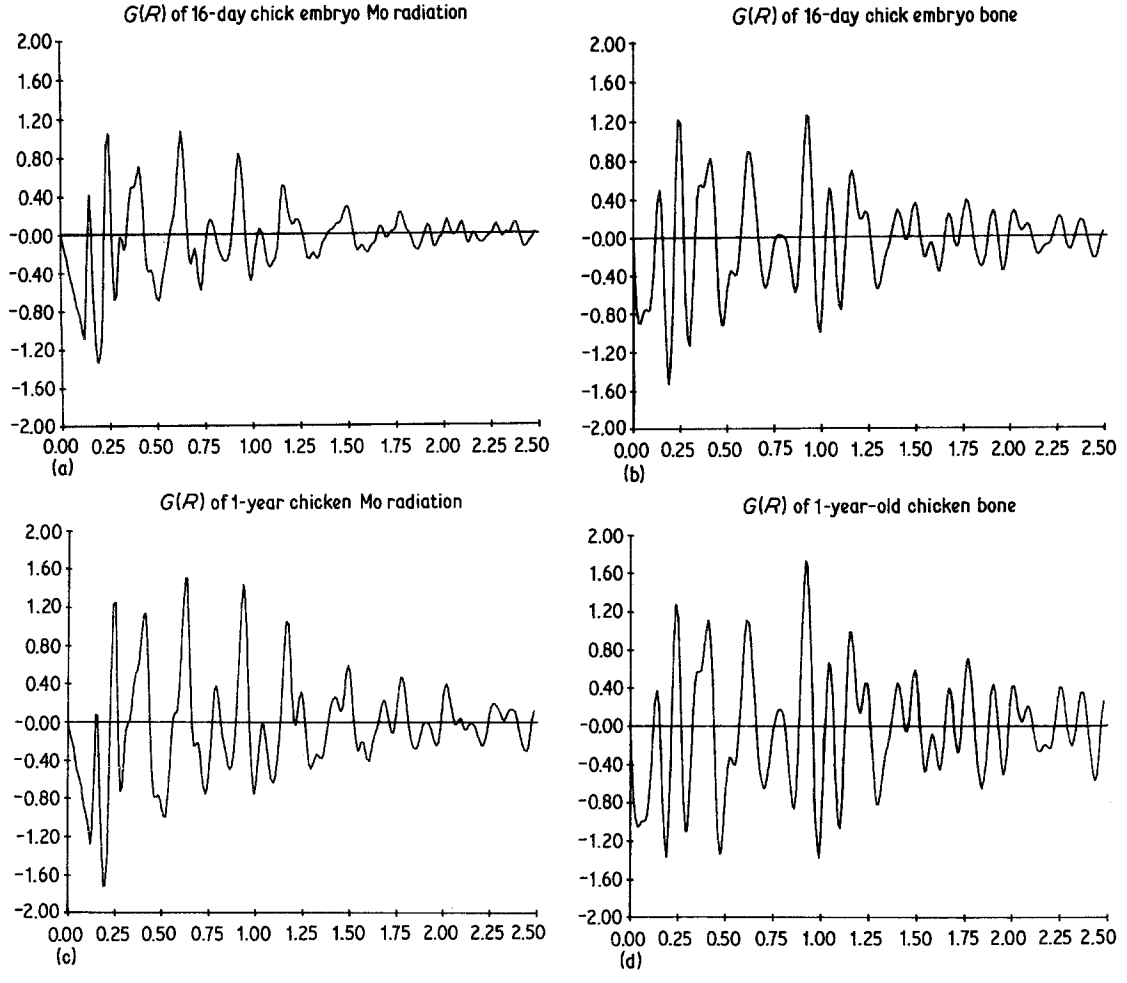

Figure 5 RDFs [$G(R)$ against R in nm] of 16-day chick embryo bone and 1-year-old chicken bone calculated from data collected with molybdenum radiation (left) and copper radiation (right).

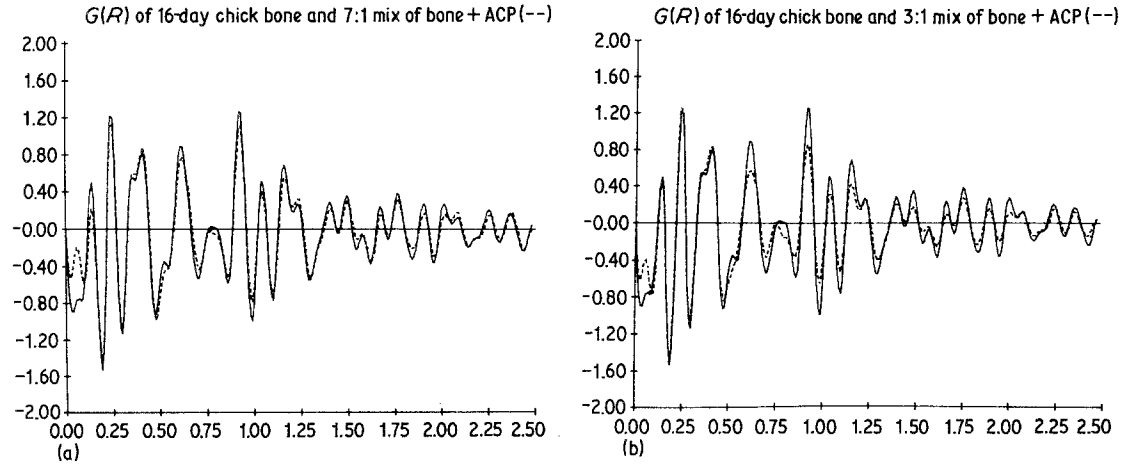

Figure 6 RDFs [$G(R)$ against R in nm] of: top, 7:1 mixture of bone and ACP (dotted line) and 16-day chick bone (solid line); and bottom, 3:1 mixture of bone and ACP (dotted line) and 16-day chick bone (solid line).

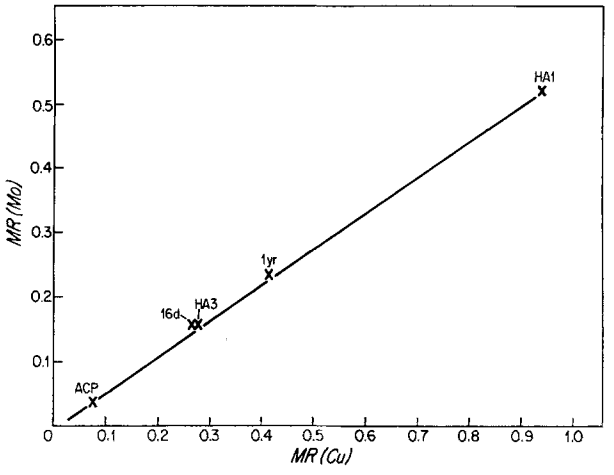

Figure 7 Modulation ratio (MR) calculated from data taken with molybdenum radiation against MR calculated from data taken with copper radiation.

significant amount of ACP in bone would be expected to produce an MR value considerably lower than expected on the basis of crystallinity or line broadening. This is confirmed by the readily detectable decreases in MR of embryonic chick bone upon the addition of 25% and 12.5% synthetic ACP. Thus the analysis of $G(r)$ does not indicate the presence of any amorphous phase in bone mineral.

Since any phase present will contribute to $G(r)$ in proportion to amount present, we conclude there is no detectable ACP in bone, even in the newly formed embryonic bone, less than 48 to 72-h-old [34], where the maximum amount of any amorphous constituent would be expected. The threshold of detectability of ACP is 12.5% or lower.

In addition, comparison of $G(r)$s and MR values of bone from embryonic and older chicks gives no indication of change in proportion of an amorphous phase with age. Thus changes in the relative proportion of ACP present cannot explain changes observed in the X-ray diffraction pattern of bone with age [2].

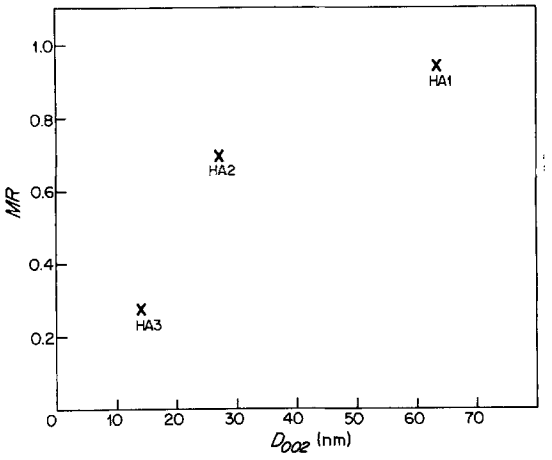

Figure 8 MR plotted against apparent crystal size D_{002} of various HA preparations.

From the earliest studies based on the ACP hypothesis, it was apparent that the diffracted intensities of synthetic "crystalline" HA used as a standard to compare with measurements obtained from bone tissue, was not a constant but was affected by variations in chemical composition and crystallite size and crystallinity. Harper and Posner [7] pointed out the necessity of using an HA standard with a crystallite size/strain parameter, as determined by the width of the [0 0 2] HA reflection, which matched that of the sample under investigation. Later, Termine *et al.* [9] showed that incorporation of CO_3 into HA standards in amounts similar to those reported from bone mineral, or the presence of surface-adsorbed ions [10], resulted in lower X-ray diffraction intensities and, therefore, led to substantially lower apparent ACP contents when these modified standards were used in the calculations. Indeed, it may be argued that if the standard used were to match bone mineral perfectly, there would be no discrepancy between the X-ray diffraction intensity of bone mineral and the standard.

Posner and Betts [19] determined the $G(r)$ of a 2:1 mixture of HA and synthetic ACP, and observed a close similarity between the RDFs of the bone mineral sample and HA. They found the fall-off in RDF peak amplitude with increasing r to be greater for the 2:1 HA + ACP mixture than for the bone mineral sample, and concluded from this that the mature bone mineral studied contained no significant amount of ACP. Because of

minor differences in the RDFs of the synthetic HA with various CO_3 contents, and indeterminacies inherent in the RDF method, they estimated that, based on their RDF data, the maximum amount of ACP, if any, which could be present in bone is 10%. More recently, Blumenthal *et al.* [35] have concluded that the RDF of mature bone can be simulated by a synthetic calcium deficient CO_3-containing hydroxyapatite containing no ACP.

We have extended the use of RDF analysis in this and other studies [20, 21] to bone of a wide range of age and extent of mineralization to determine whether bone mineral at different stages of mineralization would show changes in local atomic order as a function of tissue maturation and, in particular, whether any evidence could be found for the presence of ACP in bone mineral at any age or stage of development. We found that the RDF technique is capable of detecting small amounts (12.5%) of ACP in bone samples containing very poorly crystalline HA, and that no ACP is detectable in bone mineral, even in the youngest bone sample where most of the bone crystallites are probably no older than 48 to 72 h [34].

It is possible, of course, that there is a transient ACP phase intermediate in the formation of bone mineral which cannot be detected by RDF because its lifetime is too short or because it appears in too small quantities. Such a minor, transitory phase could not account for the changes in structure and chemistry seen in bone mineral during its maturation and ageing.

The ACP hypothesis has been useful as an attempt to explain the changes occurring in bone mineral with age, and in focusing attention on quantitative measures of changes in bone mineral crystallinity. However, further investigation has shown it to be incorrect. The X-ray diffraction pattern and chemical composition of bone mineral and the changes in these parameters observed with age and maturation of bone as a tissue and in bone mineral *per se* cannot be explained by the presence and gradual decrease of an amorphous calcium phosphate phase. The compositional and structural changes in bone mineral are consistent with a general increase in crystal size and perfection of a hydroxyapatite-like phase, although the exact details of the chemical and structural changes taking place with maturation and ageing are not known and will continue to be the subject of further research.

Acknowledgements

This work was supported in part by grants from the National Institutes of Health (AM 15671, AM 26843), the New England Home for Crippled Children, Inc, and a generous gift from the Liberty Mutual Insurance Co, and for MDG a National Institutes of Health post-doctoral fellowship (AM 16130). We gratefully acknowledge the dedicated technical assistance of Judith Blech Slyper, Irene Grubliauskas and Cynthia L. Lane.

References

1. M. J. GLIMCHER, "Handbook of Physiology: Endocrinology", Vol. 7, edited by R. O. Greep and E. B. Astwood (American Physiological Society, Washington, DC, 1976) pp. 25–113.
2. L. C. BONAR, A. H. ROUFOSSE, W. K. SABINE, M. D. GRYNPAS and M. J. GLIMCHER, *Calcif. Tissue Int.* **35** (1983) 202.
3. J. MENCZEL, A. S. POSNER and R. A. HARPER, *Isr. J. Med. Sci.* **1** (1965) 251.
4. E. D. EANES, R. A. HARPER, I. H. GILLESSEN and A. S. POSNER, "Fourth European Symposium on Calcified Tissues", edited by P. J. Gaillard, A. van der Hoof and R. Steendyk (Excerpta Medica, Amsterdam, 1966) pp. 24–26.
5. J. D. TERMINE, PhD thesis, Cornell University, Ithaca, NY, (1966).
6. E. D. EANES, I. H. GILLESSEN and A. S. POSNER, *Nature* **208** (1965) 365.
7. R. A. HARPER and A. S. POSNER, *Proc. Soc. Exptl Biol. Med.* **122** (1966) 137.
8. J. D. TERMINE and A. S. POSNER, *Calcif. Tissue Res.* **1** (1967) 8.
9. J. D. TERMINE, E. D. EANES, D. J. GREENFIELD, M. U. NYLEN and R. A. HARPER, *ibid.* **12** (1973) 73.
10. J. D. TERMINE and E. D. EANES, *ibid.* **10** (1972) 171.
11. M. QUINAUX and L. J. RICHELLE, *Isr. J. Med. Sci.* **3** (1967) 677.
12. M. D. GRYNPAS, *J. Mater. Sci.* **11** (1976) 1691.
13. C. A. BAUD, J. A. POUEZAT and H. J. TOCHON-DANGUY, "Proceedings of the 11th European Symposium on Calcified Tissues, Elsinore, 1975", edited by S. P. Nielsen and E. Hjirting-Hansen (Fadl, Copenhagen, 1976) pp. 454–6.
14. J. E. RUSSELL, J. D. TERMINE and L. V. AVIOLI, *J. Clin. Invest.* **52** (1973) 2848.
15. N. C. BLUMENTHAL, F. BETTS and A. S. POSNER, *Calcif. Tissue Int.* **23** (1977) 245.
16. J. L. MEYER and E. D. EANES, *Calcif. Tissue Res.* **25** (1978) 59.
17. J-C. HEUGHEBAERT and G. MONTEL, *Calcif. Tissue Int.* **34** (1982) S103.
18. F. BETTS and A. S. POSNER, *Mater. Res. Bull.* **9** (1974) 353.
19. A. S. POSNER and F. BETTS, *Accounts Chem. Res.* **8** (1975) 273.
20. M. J. GLIMCHER, L. C. BONAR, M. D. GRYNPAS,

W. J. LANDIS and A. H. ROUFOSSE, *J. Crystal Growth* **53** (1981) 100.
21. M. D. GRYNPAS, L. C. BONAR and M. J. GLIMCHER, unpublished results.
22. R. L. DRYER, A. R. TAMMES and J. I. ROUTH, *J. Biol. Chem.* **225** (1957) 177.
23. H. P. KLUG and L. E. ALEXANDER, "X-ray Diffraction Procedures for Polycrystalline and Amorphous Materials", 2nd edn (John Wiley, New York, 1974) pp. 677–90.
24. C. N. J. WAGNER, *J. Noncryst. Solids* **31** (1978) 1.
25. N. C. HALDER, R. J. METZGER and C. N. J. WAGNER, *J. Chem. Phys.* **45** (1966) 1259.
26. C. N. J. WAGNER, H. OCKEN and M. L. JOSHI, *Z. Naturforsch.* **20A** (1965) 235.
27. N. NORMAN, *Acta Crystallogr.* **10** (1957) 370.
28. P. A. DOYLE and P. S. TURNER, *ibid.* **A24** (1968) 390.
29. D. T. CROMER and J. T. WABER, *ibid.* **18** (1965) 104.
30. R. KAPLOW, S. L. STRONG and B. L. AVERBACH, "Local Atomic Arrangement Studied by X-ray Diffraction," edited by J. B. Cohen and J. E. Hilliard (Gordon and Breach, New York, 1966) pp. 159–77.
31. *Idem, Phys. Rev.* **138** (1965) A1336.
32. J. R. TOWNSEND and S. ERGUN, *Carbon* **6** (1968) 19.
33. B. E. WARREN, "X-ray Diffraction" (Gordon and Breach, New York, 1969) pp. 120–50.
34. M. L. TANZER and R. D. HUNT, *J. Cell Biol.* **22** (1964) 623.
35. N. C. BLUMENTHAL, F. BETTS and A. S. POSNER, *Calcif. Tissue Int.* **33** (1981) 111.

Received 21 April
and accepted 26 April 1983